



Cite this: *New J. Chem.*, 2016, 40, 6867

## Four Pb(II) metal–organic frameworks with increasing dimensions: structural diversities by varying the ligands†

Fangna Dai,<sup>a\*</sup> Weidong Fan,<sup>a</sup> Jiahui Bi,<sup>a</sup> Qian Zhang,<sup>a</sup> XiRui Zhang,<sup>a</sup> Tuo Liang,<sup>a</sup> Xingyi Wang,<sup>a</sup> Bin Dong<sup>a</sup> and Jing Gao<sup>\*b</sup>

Three rigid, linear ligands, namely 2',5'-dimethyl-[1,1':4',1''-terphenyl]-4,4''-dicarboxylic acid ( $H_2L^1$ ), triphenyl-6,6'-dicarboxylic acid ( $H_2L^2$ ), and 2,2'-bipyridine-5,5'-dicarboxylic acid ( $H_2L^3$ ), were used for constructing metal–organic frameworks (MOFs) with Pb(II). With a similar nature of solvent conditions (DMF/EtOH, with different volumes' rates), four structurally diverse MOFs, namely, [Pb( $L^1$ )(DMF)] **1**, [Pb( $L^1$ )(DMF)] **2**, [Pb( $L^2$ )] **3**, and [Pb<sub>3</sub>( $L^3$ )<sub>2</sub>(Cl<sup>-</sup>)<sub>2</sub>] **4**, were synthesized and characterized by single-crystal X-ray diffraction, thermogravimetric analysis, elemental analysis, and powder X-ray diffraction measurements. As the numbers of the central benzene ring contained in the ligands changed from three to two, the length of the ligands varied from 15.64 Å to 10.89 Å, and steric functional groups endowed the three ligands with more variations, such as a 1D zigzag chain of **1**, a 2D wave-like layer of **2**, a 3D Pb–O–C-based layer of **3**, and a 3D Pb–O–Cl-based chain of **4**. Solid-state photoluminescence studies were carried out for all the complexes at room temperature.

Received (in Montpellier, France)  
20th December 2015,  
Accepted 27th May 2016

DOI: 10.1039/c5nj03632a

www.rsc.org/njc

## Introduction

In the past few decades, great attention has been paid to metal–organic frameworks (MOFs) as a consequence of their functional properties.<sup>1</sup> Recently, the design and study of transition metal- and lanthanide-based MOFs<sup>2</sup> have evolved enormously because of their structural diversities and potential applications in fields such as magnetism,<sup>3</sup> luminescence,<sup>4</sup> gas adsorption,<sup>5</sup> optical sensing,<sup>6</sup> catalysis,<sup>7</sup> and so on.<sup>8</sup>

The MOFs are commonly prepared through connecting transition/lanthanide metal ions with appropriate bridging ligands.<sup>9</sup> Due to the widespread use in industrial applications of Pb, a toxic heavy metal, Pb(II) ions are commonly found. However, as a main group element in the periodic table, Pb(II) ions possess more sophisticated coordination preferences and electronic properties, which brings more opportunities for new structures with interesting characteristics.<sup>10</sup> Therefore, an indepth insight into the Pb(II) coordination properties, including aspects such as the lone pair electrons, coordination

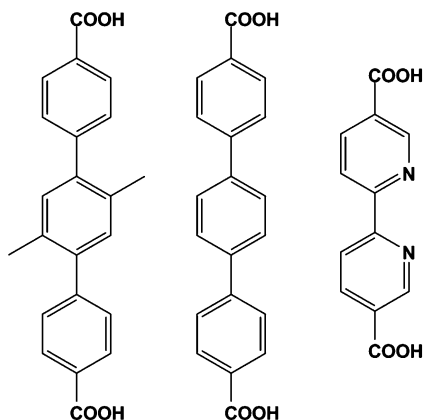
number, and coordination geometry, would be good for understanding the toxicological properties of Pb(II). In this regard, some types of architectures assembled from Pb(II) centers with aromatic carboxylates have been reported.<sup>11,12</sup> Therefore, there is great significance in continuing to explore new Pb(II) MOFs and to developing their potential applications.<sup>13,14</sup>

As we know, the synthetic process is controlled by various factors, such as the metal centers, organic ligands, pH, solvents, temperature, and auxiliary ligands,<sup>15–17</sup> of which the rational selection of the ligands and metal ions in the right solvents are important factors and can influence the crystal growth rate and the final structures.<sup>18,19</sup> In our attempt to investigate the design and control of the self-assembly of MOFs with flexible or rigid ligands, various complexes with interesting structures have been successfully isolated.<sup>20</sup> As a continuation of our work, we designed a new series of symmetrically multidentate bridging ligands (Scheme 1), namely 2',5'-dimethyl-[1,1':4',1''-terphenyl]-4,4''-dicarboxylic acid ( $H_2L^1$ ), triphenyl-6,6'-dicarboxylic acid ( $H_2L^2$ ), and 2,2'-bipyridine-5,5'-dicarboxylic acid ( $H_2L^3$ ). In particular, as members of the benzenepolycarboxylic acid family,<sup>21</sup> the above three dicarboxylate ligands, with different lengths and steric functional groups, have attracted our research interest owing to their excellent characteristics and performances, such as: (I) possessing multi-functional carboxyl groups and N-containing pyridine functional groups possessing high symmetry, which can lead to rich coordination modes and the ability to form high-dimensional structures; (II) possessing a six-membered ring that

<sup>a</sup> State Key Laboratory of Heavy Oil Processing, College of Science, China University of Petroleum (East China) Qingdao, Shandong, 266580, P. R. China

<sup>b</sup> School of Chemical Engineering, Zhejiang University of Technology, Hangzhou 310032, P. R. China. E-mail: fndai@upc.edu.cn, jingjg369@zjut.edu.cn

† Electronic supplementary information (ESI) available: X-ray powder diffraction analyses, and IR spectra details. CCDC 1426075–1426078 (1–4). For ESI and crystallographic data in CIF or other electronic format see DOI: 10.1039/c5nj03632a



Scheme 1 The dicarboxylate ligands involved in this study.

can act as  $\pi \cdot \cdot \pi$  or hydrogen-bond acceptors or donors to form supramolecular bonds to stabilize the coordination polymers; (III) possessing methyl groups that can act as space hindrance groups for the phenyl ring plane, making metal ions connect through different directions, thus bringing forward new structures; (IV) as the numbers of the central benzene ring contained in the ligands can change from three to two, such that the length of the ligands then varies from 15.64 Å to 10.89 Å, and the steric functional groups endow the whole ligand with more variations.

In the present paper, by the self-assembly of those ligands with Pb(II) ions, four MOFs, namely [Pb(L<sup>1</sup>)(DMF)] **1**, [Pb(L<sup>1</sup>)(DMF)] **2**, [Pb(L<sup>2</sup>)] **3**, and [Pb<sub>3</sub>(L<sup>3</sup>)<sub>2</sub>(Cl<sup>-</sup>)<sub>2</sub>] **4**, with a 1D zigzag chain of **1**, a 2D wave-like layer of **2**, a 3D Pb–O–C-based layer of **3**, and a 3D Pb–O–Cl-based chain of **4**, constructed from triphenyl or dipyridine ring ligands are reported. As the structures of these new MOFs are based on the different ligands, they exhibit remarkable diversities and unique structural features. The TGA, powder X-ray

diffraction patterns and photoluminescence properties of **1–4** are also reported.

## Materials and methods

H<sub>2</sub>L<sup>1,2</sup> were synthesized using a Suzuki coupling approach,<sup>22</sup> while H<sub>2</sub>L<sup>3</sup> was commercially purchased. Powder X-ray diffraction experiments were measured with a Bruker AXS D8 Advance instrument. The IR spectra were operated on a Nicolet 330 FTIR Spectrometer in the range of 4000–400 cm<sup>-1</sup>. Thermogravimetric experiments (TGA) were performed using a Perkin-Elmer TGA7 instrument. Photoluminescence spectra were recorded using an F-280 fluorescence spectrophotometer. Elemental analyses (C, H, and N) were carried out on a Perkin-Elmer 240 elemental analyzer.

### Crystal structure determinations

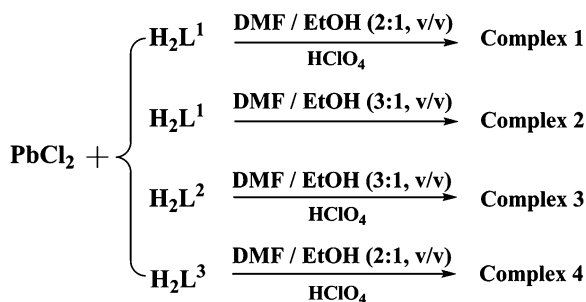
Crystallographic data for **1–4** were collected on an Agilent SuperNova diffractometer with Mo-K $\alpha$  ( $\lambda = 0.71073$  Å). All the structures were solved by the direct method using the SHELXS program of the SHELXTL package and refined by the full-matrix least-squares method with SHELXL.<sup>23</sup> The metal atoms in each complex were located from the E-maps, while other non-hydrogen atoms were located in successive difference Fourier syntheses and refined with anisotropic thermal parameters on  $F^2$ . The organic hydrogen atoms were generated geometrically (C–H: 0.96 Å). CCDC 1426075–1426078 (**1–4**) (Table 1).

### Syntheses of the complexes

**Synthesis of complex 1.** H<sub>2</sub>L<sup>1</sup> (6.9 mg, 0.02 mmol) and PbCl<sub>2</sub> (11.0 mg, 0.04 mmol) were dissolved in 1.0 mL of mixed solvents of DMF and EtOH (2 : 1, v/v) (Scheme 2). After 1 drop

Table 1 Crystallographic data and structure refinement for complexes **1–4**

| Complex  | <b>1</b>  | <b>2</b>  | <b>3</b>  | <b>4</b>  |
|--|---|---|---|---|
| Empirical formula                              | C <sub>26</sub> H <sub>20</sub> NO <sub>5</sub> Pb                  | C <sub>25</sub> H <sub>23</sub> NO <sub>5</sub> Pb                  | C <sub>20</sub> H <sub>12</sub> O <sub>4</sub> Pb                   | C <sub>24</sub> H <sub>12</sub> Cl <sub>2</sub> N <sub>4</sub> O <sub>8</sub> Pb <sub>3</sub> |
| Formula weight                                 | 633.49  | 624.63  | 523.49  | 1176.85   |
| Temperature/K                                  | 293   | 293(2)  | 200   | 293(2)  |
| Crystal system                                 | Orthorhombic  | Monoclinic  | Monoclinic  | Monoclinic  |
| Space group                                    | <i>Pnam</i>   | <i>I2/c</i>   | <i>I2/c</i>   | <i>C2/c</i>   |
| <i>a</i> /Å                                    | 8.9739(6)   | 16.7340(6)  | 7.7028(3)   | 19.6153(5)  |
| <i>b</i> /Å                                    | 8.5841(6)   | 8.0020(2)   | 5.3856(2)   | 7.10613(16)   |
| <i>c</i> /Å                                    | 30.686(3)   | 34.8764(9)  | 35.9661(15)   | 18.5113(4)  |
| $\alpha$ /°                                    | 90.00   | 90.00   | 90  | 90.00   |
| $\beta$ /°                                     | 90.00   | 101.383(3)  | 95.458(4)   | 94.072(2)   |
| $\gamma$ /°                                    | 90.00   | 90.00   | 90  | 90.00   |
| Volume/Å <sup>3</sup>                          | 2363.9(3)   | 4578.3(2)   | 1485.25(10)   | 2573.76(11)   |
| <i>Z</i>                                       | 4   | 8   | 4   | 4   |
| $\rho_{\text{calc}}/\text{mg mm}^{-3}$         | 1.854   | 1.812   | 2.341   | 3.037   |
| $\mu/\text{mm}^{-1}$                           | 7.179   | 7.406   | 11.383  | 19.843  |
| <i>F</i> (000)                                 | 1272.0  | 2416.0  | 984.0   | 2112.0  |
| Radiation                                      | MoK $\alpha$ ( $\lambda = 0.71073$ )                                | MoK $\alpha$ ( $\lambda = 0.71073$ )                                | MoK $\alpha$ ( $\lambda = 0.71073$ )                                | MoK $\alpha$ ( $\lambda = 0.71073$ )  |
| $2\theta$ range for data collection            | 6.24 to 52°   | 5.912 to 52.686°  | 6.828 to 57.836°  | 5.84 to 52.68°  |
| Reflections collected                          | 5744  | 9829  | 5131  | 5451  |
| Independent reflections                        | 2101 [ $R_{\text{int}} = 0.0626$ ,<br>$R_{\text{sigma}} = 0.0857$ ] | 4664 [ $R_{\text{int}} = 0.0282$ ,<br>$R_{\text{sigma}} = 0.0425$ ] | 1742 [ $R_{\text{int}} = 0.0452$ ,<br>$R_{\text{sigma}} = 0.0523$ ] | 2623 [ $R_{\text{int}} = 0.0371$ ,<br>$R_{\text{sigma}} = 0.0520$ ]                           |
| Data/restraints/parameters                     | 2101/27/169   | 4664/467/420  | 1742/0/114  | 2623/0/186  |
| Goodness-of-fit on $F^2$                       | 1.004   | 1.048   | 1.078   | 1.063   |
| Final <i>R</i> indexes [ $I \geq 2\sigma(I)$ ] | $R_1 = 0.0446$ , $wR_2 = 0.0740$                                    | $R_1 = 0.0315$ , $wR_2 = 0.0568$                                    | $R_1 = 0.0268$ , $wR_2 = 0.0539$                                    | $R_1 = 0.0332$ , $wR_2 = 0.0650$  |



Scheme 2 The solvent conditions involved in this study.

of perchloric acid was added, the resulting solution was sealed in a glass tube, heated to 130 °C at a rate of 15 °C h<sup>-1</sup>, kept at 130 °C for 90 h, and then cooled to room temperature at a rate of 15 °C h<sup>-1</sup>. The resulting colorless needle-shaped crystals of **1** were collected by filtration, washed several times with DMF and EtOH, and dried in the air (yield: 25%). Elemental anal. calcd for **1**: C, 48.15; H, 3.55; N, 2.25%; found: C, 48.32; H, 3.75; N, 2.41%.

**Synthesis of complex 2.**  $\text{H}_2\text{L}^1$  (6.9 mg, 0.02 mmol) and  $\text{PbCl}_2$  (11.0 mg, 0.04 mmol) were dissolved in 1.0 mL of mixed solvents of DMF and EtOH (3:1, v/v), the resulting solution was sealed in a glass tube, heated to 130 °C at a rate of 15 °C h<sup>-1</sup>, kept at 130 °C for 90 h, and then cooled to room temperature at a rate of 15 °C h<sup>-1</sup>. The resulting colorless needle-shaped crystals of **2** were collected by filtration, washed several times with DMF and EtOH, and dried in the air (yield: 30%). Elemental anal. calcd for **2**: C, 49.25; H, 3.16; N, 2.21%; found: C, 48.03; H, 3.68; N, 2.24%.

**Synthesis of complex 3.**  $\text{H}_2\text{L}^2$  (6.4 mg, 0.02 mmol) and  $\text{PbCl}_2$  (11.0 mg, 0.04 mmol) were dissolved in 1.0 mL of mixed solvents of DMF and EtOH (3:1, v/v). After 1 drop of perchloric acid was added, the resulting solution was sealed in a glass tube, heated to 130 °C at a rate of 15 °C h<sup>-1</sup>, kept at 130 °C for 90 h, and then cooled to room temperature at a rate of 15 °C h<sup>-1</sup>. The resulting colorless needle-shaped crystals of **3** were collected by filtration, washed several times with DMF and EtOH, and dried in the air (yield: 29%). Elemental anal. calcd for **3**: C, 45.86; H, 2.31%; found: C, 45.04; H, 2.64%.

**Synthesis of complex 4.**  $\text{H}_2\text{L}^3$  (4.9 mg, 0.02 mmol) and  $\text{PbCl}_2$  (11.0 mg, 0.04 mmol) were dissolved in 1.0 mL of mixed solvents of DMF and EtOH (2:1, v/v). After 1 drop of perchloric acid was added, the resulting solution was sealed in a glass tube, heated to 130 °C at a rate of 15 °C h<sup>-1</sup>, kept at 130 °C for 90 h, and then cooled to room temperature at a rate of 15 °C h<sup>-1</sup>. The resulting colorless needle-shaped crystals of **4** were collected by filtration, washed several times with DMF and EtOH, and dried in the air (yield: 45%). Elemental anal. calcd for **4**: C, 24.49; H, 1.03; N, 4.76%; found: C, 24.74; H, 1.31; N, 4.63%.

## Results and discussion

### 1D zigzag chain of complex 1

Single-crystal X-ray diffraction revealed that complex **1** crystallizes in the orthorhombic space group *Pnam*, and that the

asymmetric unit consists of half of one  $\text{Pb}^{2+}$  ion, half of one  $\text{L}^1$  ligand, and half of one coordinated DMF molecule. There is only half of complex in the asymmetry unit, but another half part could be generated by an inversion center. The central  $\text{Pb}^{2+}$  ion is five-coordinated by four oxygen atoms from two  $\text{L}^1$  ligands and one oxygen atoms from the coordinated DMF molecule, with an average Pb–O distance of 2.502 Å. Both carboxylate groups of  $\text{L}^1$  are deprotonated during the reaction, and adopt a bidentate chelating mode to chelate one  $\text{Pb}^{2+}$  ion (Fig. 1a). The average dihedral angle between the side benzene ring and the central benzene ring is 64.264°. The whole ligand acts as a bridging linker to connect  $\text{Pb}^{2+}$  ions into a 1D zigzag chain (Fig. 1b), in which all  $\text{Pb}^{2+}$  ions are exactly in a planar arrangement, with the coordinated DMF molecules hanging in the vertical opposite direction of the plane. The 1D zigzag chains are connected into 3D structures by weak C–H···O intramolecular H-bonds (3.144 Å and 3.603 Å) (Fig. 1c).

### 2D wave-like layer of complex 2

Single-crystal X-ray diffraction revealed that complex **2** crystallizes in the monoclinic space group *I2/c*, and that the asymmetric unit consists of one  $\text{Pb}^{2+}$  ion, one  $\text{L}^1$  ligand, and one coordinated DMF molecule. The  $\text{Pb}^{2+}$  ion is five-coordinated by six oxygen atoms from four  $\text{L}^1$  ligands, and one oxygen atom from the coordinated DMF molecule, with an average Pb–O distance of 2.538 Å. Both carboxylate groups of  $\text{L}^1$  are deprotonated during the reaction, and adopt a tridentate bridging chelating mode to connect  $\text{Pb}^{2+}$  ions (Fig. 2a). The average dihedral angle between the side benzene rings and the central benzene ring is 56.429° and 52.671°, respectively, as shown in Fig. 2a. The  $\text{Pb}^{2+}$  ions are connected by the oxygen atoms from the  $\text{L}^1$  ligands to form infinite Pb–O–Pb second building units (SBUs) (Fig. 2b), and the whole ligand acts as a bridging linker to connect Pb ions into a

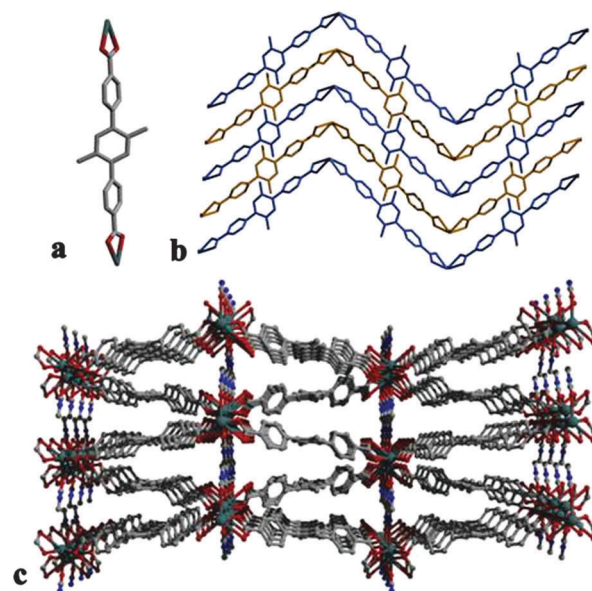


Fig. 1 (a) Chelating mode of  $\text{L}^1$ ; (b) and (c) 1D zigzag chain and 3D structure of **1**.



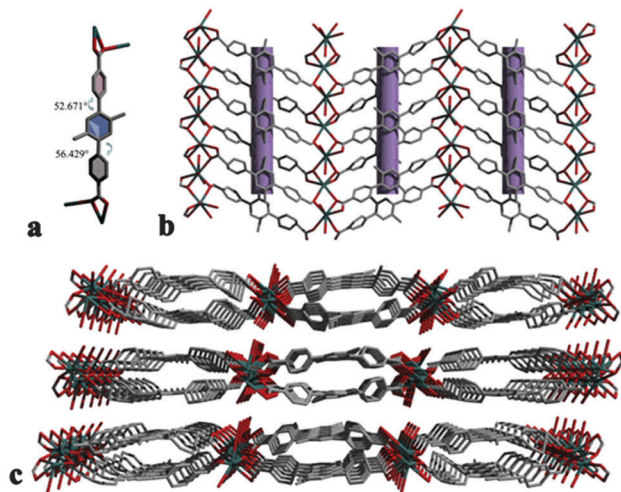


Fig. 2 (a) Coordination mode of  $L^1$ ; (b) and (c) 2D wave-like layer and 3D structures of **2**, respectively.

2D wave-like layer containing a 34-membered ring (Fig. 2b). The 2D wave-like layers are further connected into 3D (Fig. 2c) structures by weak C-H...O intramolecular H-bonds (3.376 Å).

### 3D porous structures of complexes **3** and **4**

Single-crystal X-ray diffraction revealed that complex **3** crystallizes in the monoclinic space group  $I2/c$ , and that the asymmetric unit of **3** consists of half of one  $Pb^{2+}$  ion and half of one  $L^2$  ligand. The  $Pb^{2+}$  ion, which lies in a 2-fold axis, is six-coordinated by six oxygen atoms from six  $L^2$  ligands, with an average Pb–O distance of 2.548 Å. Both carboxylate groups of  $L^2$  are deprotonated during the reaction, and adopt a tridentate bridging chelating mode to connect  $Pb^{2+}$  ions (Fig. 3a), which is the same as in complex **2**. The average dihedral angle between the side benzene ring and the central benzene ring is 4.148°, much smaller than that for complexes **1** and **2** obviously. The  $Pb^{2+}$  ions are connected by the oxygen atoms from the  $L^2$

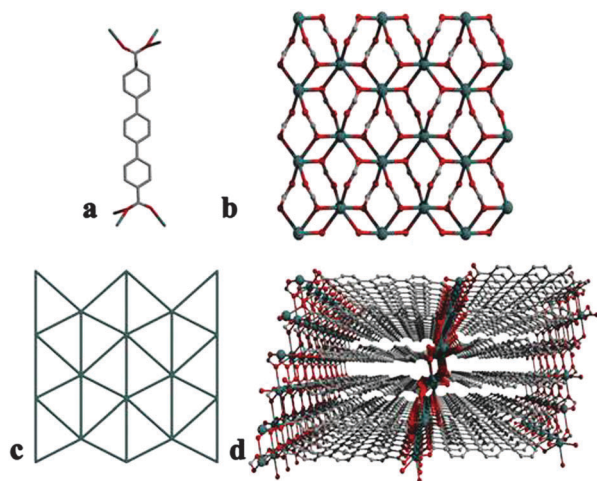


Fig. 3 (a) Coordination mode of  $L^2$ ; (b) 2D Pb–O–Pb layer of **3**; (c) and (d) simplifications of the 2D Pb–O–Pb layer and 3D structure of **3**.

ligands to form an infinite Pb–O–Pb layer (Fig. 3b and c), and the whole ligand acts as a bridging linker to connect the 2D Pb layers into a 3D structure (Fig. 3d).

Single-crystal X-ray diffraction revealed that complex **4** crystallizes in the monoclinic space group  $C2/c$ , and that the asymmetric unit consists of one and a half  $Pb^{2+}$  ions, one  $L^3$  ligand, and one coordinated  $Cl^-$ . The central Pb1 ion is seven-coordinated by four oxygen atoms from three  $L^3$  ligands, one coordinated  $Cl^-$ , and two nitrogen atoms from a fourth  $L^3$  ligand, with an average Pb–O distance of 2.778 Å, Pb–Cl distance of 2.738 Å, and Pb–N distance of 2.652 Å. Pb2 is eight-coordinated by six oxygen atoms from four  $L^3$  ligands and two coordinated  $Cl^-$ , with an average Pb–O distance of 2.664 Å and Pb–Cl distance of 2.981 Å. Thus, the  $Pb^{2+}$  ions are connected by oxygen atoms and  $Cl^-$  to form infinite Pb–O–Cl SBUs (Fig. 4b). Both carboxylate groups of  $H2L^3$  are deprotonated during the reaction, of which one adopts a tridentate bridging chelating mode and the other one adopts a four-dentate bridging chelating mode to connect  $Pb^{2+}$  ions. The nitrogen atoms from the  $L^3$  ligand adopts a bidentate chelating mode to chelate one  $Pb^{2+}$  ion (Fig. 4a). The dihedral angle between the two benzene rings is 3.678°, which means they are nearly coplanar to each other. The whole ligand acts as a bridging linker to connect the Pb–O–Cl SBUs into a 3D structure (Fig. 4c). It is worth noting that there are weak intramolecular C5–H...Cl1 (3.746 Å) and C8–H...Cl1 (3.611 Å) bonds in complex **4**.

### X-ray powder diffraction analyses, IR spectra, thermal analyses and luminescent properties

Once isolated, all of the complexes were stable in air and insoluble in common organic solvents and water. PXRD was used to check the purity of the samples in the solid state. The measured PXRD patterns of the four complexes highly matched the simulated ones generated from the results of the single-crystal diffraction data by the Mercury program, indicating they were all pure products (Fig. S1, ESI<sup>†</sup>). The IR spectra of complexes **1–4** show sharp bands in the ranges of 1700–1550 and 1400–1300  $cm^{-1}$ , which are due to the asymmetric and symmetric stretching vibrations of the carboxylate groups, respectively.<sup>24</sup> Broad peaks in the range of 3363–3465  $cm^{-1}$  for the spectra of the ligand can be attributed to the vibration of O–H from carboxyl, while for the spectra of the two complexes,

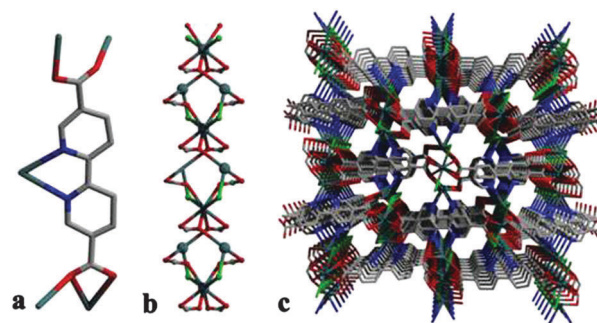


Fig. 4 (a) Coordination mode of  $L^3$ ; (b) and (c) Pb–O–Cl SBUs and 3D structures of **4**.

they can be ascribed to O–H stretch of lattice and uncoordinated ethanol molecules.<sup>25</sup> These results were also established by single-crystal analysis (Fig. S2, ESI†).

The thermogravimetric analysis (TGA) experiments were performed in a N<sub>2</sub> atmosphere with a heating rate of 10 °C min<sup>-1</sup> on polycrystalline samples of complexes 1–4. The TGA curves are shown in Fig. 5. For complex 1, from 25 to 290 °C, the weight loss of 11.65% is equivalent to the loss of coordinated DMF molecules (calculated: 11.7%). Upon further heating, 1 starts to decompose. For complex 2, from 25 to 330 °C, the weight loss of 11.78% is attributed to the loss of coordinated DMF molecules (calculated: 11.7%); upon further heating, 2 starts to decompose. For complex 3, the gradual weight loss from 50 to 120 °C is in accordance with the loss of surface uncoordinated ethanol molecules. 3 could be stable up to 400 °C, after that, the decomposition starts. The TGA curve of complex 4 shows it could be stable up to 370 °C, after that, the framework starts to decompose. It is notable that the higher thermal stabilities of complexes 3 and 4 could be attributed to the 2D layer Pb–O–Pb SBUs of 3 and Pb–O–Cl SBUs of 4, respectively, which is in line with the previous published reports that the SBUs could enhance the stability of MOF structures.<sup>26</sup>

MOFs always show varied luminescent properties, leading to their potential applications in photochemistry, chemical sensors, and electroluminescent displays. Compared to traditional transition or lanthanide metals, d<sup>10</sup> transition metal complexes are usually promising candidates to exhibit photoluminescent properties,<sup>27</sup> and the emission wavelength and luminescent theory are always affected by the coordination modes of the organic ligands and metals.<sup>28</sup>

In the present work, the solid-state photoluminescent spectra of H<sub>2</sub>L<sup>1–3</sup>, and complexes 1–4 were measured at room temperature (Fig. 6). The H<sub>2</sub>L<sup>1</sup> ligand displays photoluminescence with emission maxima at 404 nm ( $\lambda_{\text{ex}} = 408$  and 350 nm), which can be presumed to relate to the  $\pi^* \rightarrow n$  or  $\pi^* \rightarrow \pi$  transitions.<sup>29</sup> The emission band shows a lesser blue-shift to 398 nm ( $\lambda_{\text{ex}} = 330$  nm) for 1, and a lesser red-shift to 411 nm ( $\lambda_{\text{ex}} = 350$  nm) for 2 in comparison with those of H<sub>2</sub>L<sup>1</sup> ligand. The H<sub>2</sub>L<sup>2</sup> ligand displays photoluminescence with emission maximum at 409 nm and

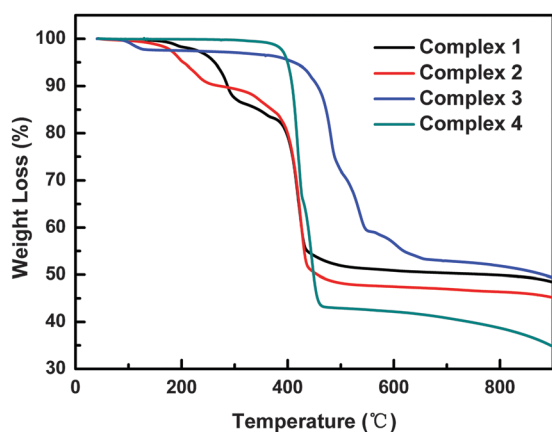


Fig. 5 TGA curves of 1–4.

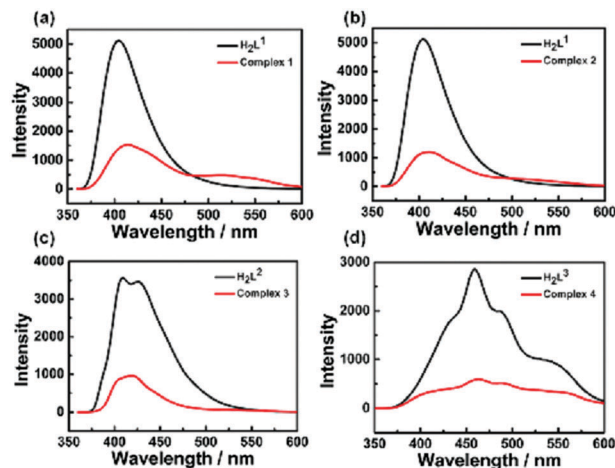


Fig. 6 Solid-state photoluminescent spectra of H<sub>2</sub>L<sup>1–3</sup> and complexes 1–4.

426 nm ( $\lambda_{\text{ex}} = 347$ ). It should be noted that the emission peaks become a single peak and the maximum peaks are at 414 nm ( $\lambda_{\text{ex}} = 352$  nm) for 3. Complex 4 maintains a similar shape compared with that of the H<sub>2</sub>L<sup>3</sup> ligand, which displays photoluminescence, with an emission maxima at 460 nm ( $\lambda_{\text{ex}} = 330$  nm), while the maximum peaks are at 463 nm ( $\lambda_{\text{ex}} = 330$  nm) for 4. We can see that all the photoluminescence of the four complexes maintain a similar shape and are changed little compared to their starting ligands. The emission of the complexes can be attributed to ligand-to-metal charge transfer (LMCT) between the delocalized  $\pi$ -bond of the carboxylate groups and p orbitals of the Pb(II) centers.<sup>30</sup>

#### Effects of the H<sub>2</sub>L<sup>1–3</sup> ligand on the dimensions of the MOFs

It is well-known that the dihedral angles come from rotation of the C–C bonds to match the requirements of coordination.<sup>30</sup> For L<sup>1–3</sup> ligands, in addition to the different lengths (from 15.64 Å to 10.89 Å) caused by the different numbers of contained aromatic rings, there exist different coordination modes and dihedral angles of the aromatic rings. In complexes 1–4, the carboxylic groups adopt different coordinate modes:  $\mu_2: \eta_1: \eta_1: \eta_1: \eta_1$  for 1,  $\mu_4: \eta_1: \eta_2: \eta_2: \eta_1$  for 2,  $\mu_6: \eta_1: \eta_2: \eta_1: \eta_2$  for 3 and  $\mu_5: \eta_1: \eta_1: \eta_1: \eta_1: \eta_1: \eta_2$  for 4. The dihedral angle between the side benzene ring and the central benzene ring varied from 64.264° in complex 1 to 59.904° and 52.156° in complex 2, which correspond to a 1D layer structure for 1 and a 2D wave-like structure for 2. In complex 3, the dihedral angle between the side benzene ring and the central benzene ring is 4.152°, which is obviously smaller than that in complexes 1 and 2, and the coordination modes are more open in complex 3 than that in complexes 1 and 2, leading to 3D structures for 3. The average dihedral angle between two pyridine rings is 1.302°, and there are two more coordination sites in complex 4, leading to a 3D structure. The coordination of Cl<sup>-</sup> anions to Pb(II) may be responsible for the quite small dihedral angle. As every ligand connects to six or five metal ions, they are more thermally stable for complexes 3 and 4. In other words, the coordination modes of the ligands significantly affect the number of coordinated oxygen atoms

around the metal ion, which further results in the structural diversity of the final structures and thermal stability. In addition, for 1–4, they were prepared under the same hydro(solvo)thermal condition except with different solvent conditions (DMF:EtOH, v:v = 3:1–2:1). However, the resultant structures are absolutely different, which further proves the important role of the solvent conditions in modulating the final structural motifs.

## Conclusions

In summary, four Pb-MOFs based on three rigid, linear ligands were obtained and characterized by elemental analysis, single-crystal X-ray crystallography, powder X-ray diffraction, infrared spectroscopy, and thermogravimetric analyses. As the number of central benzene rings contained in the ligands changed from three to two, the length of the ligands varies from 15.64 Å to 10.89 Å and steric functional groups endow the whole ligand with variations. There are a 1D zigzag chain of 1, a 2D wave-like layer of 2, a 3D Pb–O–C-based layer of 3, and a Pb–O–Cl-based chain of 4. Solid-state photoluminescence studies were carried out for all of the complexes in the solid state at room temperature.

## Acknowledgements

This work was supported by the NSFC (Grant No. 21301154, 21201179 and 21173193), the Fundamental Research Funds for the Central Universities (14CX02213A, 16CX05015A), and the Foundation of State Key Laboratory of Structural Chemistry (20160006).

## References

- (a) J. R. Li, R. J. Kuppler and H. C. Zhou, *Chem. Soc. Rev.*, 2009, **38**, 1477; (b) S. Hausdorf, F. Baitalow, T. Bohle, D. Rafaja and F. O. R. L. Mertens, *J. Am. Chem. Soc.*, 2010, **132**, 10978; (c) C. Wang, Z. Xie, K. E. deKrat and W. Lin, *J. Am. Chem. Soc.*, 2011, **133**, 13445; (d) C. F. Hansell, P. Espeel, M. M. Stamenovic, I. A. Barker, A. P. Dove, F. E. Du Prez and R. K. O'Reilly, *J. Am. Chem. Soc.*, 2011, **133**, 13828; (e) A. D. Burrows, L. C. Fisher, C. Richardson and S. P. Rigby, *Chem. Commun.*, 2011, **47**, 3380.
- (a) L. Q. Ma, C. Abney and W. B. Lin, *Chem. Soc. Rev.*, 2009, **38**, 1248; (b) J. Q. Sha, J. W. Sun, C. Wang, G. M. Li, P. F. Yan and M. T. Li, *Cryst. Growth Des.*, 2012, **12**, 2242; (c) T. Antonio, G. B. Robert and M. D. Caroline, *Cryst. Growth Des.*, 2010, **10**, 2839; (d) N. Stock and S. Biswas, *Chem. Rev.*, 2012, **112**, 933.
- (a) J. W. Liu, L. F. Chen, H. Cui, J. Y. Zhang, L. Zhang and C. Y. Su, *Chem. Soc. Rev.*, 2014, **43**, 60; (b) E. I. Vasylev'sky, G. A. Senchyk, A. B. Lysenko, E. B. Rusanov, A. N. Chernega, J. Jezierska, H. Krautscheid, K. V. Domasevitch and A. Ozarowski, *Inorg. Chem.*, 2014, **53**, 3642; (c) E. Coronado and G. M. Espallargas, *Chem. Soc. Rev.*, 2013, **42**, 1525.
- (a) S. Zhang, Y. Yang, Z. Q. Xia, X. Y. Liu, Q. Yang, Q. Wei, G. Xie, S. P. Chen and S. L. Gao, *Inorg. Chem.*, 2014, **53**, 10952; (b) M. D. Allendorf, C. A. Bauer, R. K. Bhakta and R. J. T. Houk, *Chem. Soc. Rev.*, 2009, **38**, 1330; (c) L. N. Jia, L. Hou, L. Wei, X. J. Jing, B. Liu, Y. Y. Wang and Q. Z. Shi, *Cryst. Growth Des.*, 2013, **13**, 1570; (d) L. V. Meyer, F. Schönfeld and K. Müller-Buschbaum, *Chem. Commun.*, 2014, **50**, 8093; (e) V. I. Isaeva, E. V. Belyaeva, A. N. Fitch, V. V. Chernyshev, S. N. Klyamkin and L. M. Kustov, *Cryst. Growth Des.*, 2013, **13**, 5305.
- (a) H. J. Sung, A. K. Nazmul and H. Zubair, *CrystEngComm.*, 2012, **14**, 7099; (b) R. Dawson, D. J. Adams and A. I. Cooper, *Chem. Sci.*, 2011, **2**, 1173; (c) A. J. Calahorra, A. Peñas-Sanjuan, M. Melguizo, D. Fairen-Jimenez, G. Zaragoza, B. Fernández, A. Salinas-Castillo and A. Rodríguez-Diéguez, *Inorg. Chem.*, 2013, **52**, 546; (d) Y. B. He, B. Li, M. O'Keeffe and B. L. Chen, *Chem. Soc. Rev.*, 2014, **43**, 5618; (e) D. W. Andrew, G. Christophe, V. Dominique, B. Emily, R. Helge, S. Norbert, J. S. Lee, J. S. Chang and L. L. Philip, *ACS Comb. Sci.*, 2013, **15**, 111.
- (a) X. H. Jin, J. K. Sun, X. M. Xu, Z. H. Li and J. Zhang, *Chem. Commun.*, 2010, **46**, 4695; (b) C. Y. Lee, O. K. Farha, B. J. Hong, A. A. Sarjeant, S. B. T. Nguyen and J. T. Hupp, *J. Am. Chem. Soc.*, 2011, **133**, 15858; (c) D. F. S. Gallis, L. E. S. Rohwer, M. A. Rodriguez and T. M. Nenoff, *Chem. Mater.*, 2014, **26**, 2943; (d) A. Y. Robin and K. M. Fromm, *Coord. Chem. Rev.*, 2006, **250**, 2127.
- (a) C. C. Wang, J. R. Li, X. L. Lv, Y. O. Zhang and G. S. Guo, *Energy Environ. Sci.*, 2014, **7**, 2831; (b) D. Bradshaw, A. Garai and J. Huo, *Chem. Soc. Rev.*, 2012, **41**, 2344; (c) H. Li, Z. H. Zhu, F. Zhang, S. H. Xie, H. X. Li, P. Li and X. G. Zhou, *ACS Catal.*, 2011, **1**, 1604; (d) P. García-García, M. Müller and A. Corma, *Chem. Sci.*, 2014, **5**, 2979.
- (a) H. L. Jiang and Q. Xu, *Chem. Commun.*, 2011, **47**, 3351; (b) S. L. Li and Q. Xu, *Energy Environ. Sci.*, 2013, **6**, 1656; (c) T. B. Faust and D. M. D'Alessandro, *RSC Adv.*, 2014, **4**, 17498; (d) A. Dhakshinamoorthy, M. Alvaro, A. Corma and H. Garcia, *Dalton Trans.*, 2011, **40**, 6344; (e) D. Bradshaw, A. Garai and J. Huo, *Chem. Soc. Rev.*, 2012, **41**, 2344.
- (a) Y. Q. Sun, Q. Liu, L. L. Zhou and Y. P. Chen, *CrystEngComm.*, 2014, **16**, 3986; (b) X. L. Ni, X. Xiao, H. Cong, L. L. Liang, K. Cheng, X. J. Cheng, N. N. Ji, Q. J. Zhu, S. F. Xue and Z. Tao, *Chem. Soc. Rev.*, 2013, **42**, 9480; (c) B. Zhao, X. Y. Chen, Z. Chen, W. Shi, P. Cheng, S. P. Yan and D. Z. Liao, *Chem. Commun.*, 2009, 3113; (d) D. F. S. Gallis, L. E. S. Rohwer, M. A. Rodriguez and T. M. Nenoff, *Chem. Mater.*, 2014, **26**, 2943.
- (a) J. Yang, J. F. Ma, Y. Y. Liu, J. C. Ma and S. R. Batten, *Cryst. Growth Des.*, 2009, **9**, 1894; (b) T. Devic and C. Serre, *Chem. Soc. Rev.*, 2014, **43**, 6097; (c) X. Q. Li, H. B. Zhang, S. T. Wu, J. D. Lin, P. Lin, Z. H. Li and S. W. Du, *CrystEngComm.*, 2012, **14**, 936; (d) X. M. Lin, T. T. Li, L. F. Chen, L. Zhang and C. Y. Su, *Dalton Trans.*, 2012, **41**, 10422; (e) A. Santra and P. K. Bharadwaj, *Cryst. Growth Des.*, 2014, **14**, 1476.
- (a) E. S. Claudio, H. A. Godwin and J. S. Magyar, *Prog. Inorg. Chem.*, 2003, **51**, 1; (b) A. Pellissier, Y. Bretonniere, N. Chatterton, J. Pecaut, P. Delangle and M. Mazzanti, *Inorg. Chem.*, 2007, **46**, 3714; (c) R. J. Andersen, R. C. Targiani, R. D. Hancock, C. L. Stern, D. P. Goldberg and H. A. Godwin,



- Inorg. Chem.*, 2006, **45**, 6574; (d) J. G. Mao, Z. K. Wang and A. Clearfield, *Inorg. Chem.*, 2002, **41**, 6106.
- 12 (a) B. Sui, W. Zhao, G. Ma, T. Okamura, J. Fan, Y. Z. Li, S. H. Tang, W. Y. Sun and N. Ueyama, *J. Mater. Chem.*, 2004, **14**, 1631; (b) J. E. H. Buston, T. D. W. Claridge, S. J. Heyes, M. A. Leech, M. G. Moloney, K. Prout and M. Stevenson, *Dalton Trans.*, 2005, 3195; (c) K. L. Zhang, Y. Chang, C. T. Hou, G. W. Diao and R. T. Wu, *CrystEngComm.*, 2010, **12**, 1194; (d) Y. F. Kang, J. Q. Liu, B. Liu, W. T. Zhang, Q. Liu, P. Liu and Y. Y. Wang, *Cryst. Growth Des.*, 2014, **14**, 5466.
- 13 (a) X. Q. Wang, J. Yang, L. L. Zhang, F. L. Liu, F. N. Dai and D. F. Sun, *Inorg. Chem.*, 2014, **53**, 11206; (b) J. Sun, F. N. Dai, W. B. Yuan, W. H. Bi, X. L. Zhao, W. M. Sun and D. F. Sun, *Angew. Chem., Int. Ed.*, 2011, **50**, 7061; (c) F. N. Dai, J. M. Dou, H. Y. He, X. L. Zhao and D. F. Sun, *Inorg. Chem.*, 2010, **49**, 4117.
- 14 (a) L. Lisnard, P. Mialane, A. Dolbecq, J. Marrot, J. M. Clemente Juan, E. Coronado, B. Keita, B. P. de Oliveira, L. Nadjo and F. Secheresse, *Chem. – Eur. J.*, 2007, **13**, 3525; (b) X. J. Li, X. Y. Wang, S. Gao and R. Cao, *Inorg. Chem.*, 2006, **45**, 1508; (c) J. Sahu, M. Ahmad and P. K. Bharadwaj, *Cryst. Growth Des.*, 2013, **13**, 2618.
- 15 (a) Y. Z. Tang, X. S. Wang, T. Zhou and R. G. Xiong, *Cryst. Growth Des.*, 2006, **6**, 11; (b) D. Dobrzynska, L. B. Jerzykiewicz, J. Jezierska and M. Duczmal, *Cryst. Growth Des.*, 2005, **5**, 1945; (c) J. Luo, Y. Zhao, H. Xu, T. L. Kinniburgh, D. Yang, T. V. Timofeeva, L. L. Daemen, J. Zhang, W. Bao, J. D. Thompson and R. P. Currier, *Inorg. Chem.*, 2007, **46**, 9021; (d) A. Morsali, V. T. Yilmaz, C. Kazakc and L. G. Zhu, *Helv. Chim. Acta*, 2005, **88**, 2513; (e) L. K. Li, Y. L. Song, H. W. Hou, Y. T. Fan and Y. Zhu, *Eur. J. Inorg. Chem.*, 2005, 3238.
- 16 (a) X. Zhang, C. Guo, Q. Yang, W. Wang, W. Liu, B. Kang and C. Su, *Chem. Commun.*, 2007, 4242; (b) Y. B. He, B. Li, M. O'keeffe and B. L. Chen, *Chem. Soc. Rev.*, 2014, **43**, 5618; (c) F. L. Hu, W. Wu, P. Liang, Y. Q. Gu, L. G. Zhu, H. Wei and J. P. Lang, *Cryst. Growth Des.*, 2013, **13**, 5050.
- 17 (a) S. M. Cohen, *Chem. Rev.*, 2012, **112**, 970; (b) Z. Wang and S. M. Cohen, *Chem. Soc. Rev.*, 2009, **38**, 1315.
- 18 (a) J. Park, Z. Y. U. Wang, L. B. Sun, Y. P. Chen and H. C. Zhou, *J. Am. Chem. Soc.*, 2012, **134**, 20110; (b) S. Saha, S. Santra and P. Ghosh, *Eur. J. Inorg. Chem.*, 2014, 2029; (c) L. J. Li, S. F. Tang, C. Wang, X. X. Lv, M. Jiang, H. Z. Wu and X. B. Zhao, *Chem. Commun.*, 2014, **50**, 2304.
- 19 (a) A. Y. Fu, Y. L. Jiang, Y. Y. Wang, X. N. Gao, G. P. Yang, L. Hou and Q. Z. Shi, *Inorg. Chem.*, 2010, **49**, 5495; (b) K. K. Orisaku, K. Hoshino, S. Yamashita and Y. B. Koide, *Chem. Soc. Jpn.*, 2010, **83**, 276; (c) L. Carlucci, G. Ciani, S. Maggini, D. M. Proserpio and M. Visconti, *Chem. – Eur. J.*, 2010, **16**, 12328; (d) M. C. Bernini, N. Snejkó, E. G. Puebla, E. V. Brussau, G. E. Narda and M. A. Monge, *Inorg. Chem.*, 2011, **50**, 5958.
- 20 (a) W. G. Lu, Z. W. Wei, Z. Y. Gu, T. F. Liu, J. Park, J. Tian, M. W. Zhang, Q. Zhang, T. Gentle III, M. Bosch and H. C. Zhou, *Chem. Soc. Rev.*, 2014, **43**, 5561; (b) E. Puodziukynaite, J. L. Oberst, A. L. Dyer and J. R. Reynolds, *J. Am. Chem. Soc.*, 2012, **134**, 968; (c) Z. H. Yan, W. Wang, L. L. Zhang, X. W. Zhang, L. Wang, R. M. Wang and D. F. Sun, *RSC Adv.*, 2015, **5**, 16190.
- 21 (a) S. Yuan, W. G. Lu, Y. P. Chen, Q. Zhang, T. F. Liu, D. W. Feng, X. Wang, J. S. Qin and H. C. Zhou, *J. Am. Chem. Soc.*, 2015, **137**, 3177; (b) H. L. Jiang, D. W. Feng, T. F. Liu, J. R. Li and H. C. Zhou, *J. Am. Chem. Soc.*, 2012, **134**, 14690; (c) S. Saha, S. Santra and P. Ghosh, *Eur. J. Inorg. Chem.*, 2014, 2029.
- 22 (a) X. L. Zhao, H. Y. He, F. N. Dai, D. F. Sun and Y. X. Ke, *Inorg. Chem.*, 2010, **49**, 650.
- 23 (a) Bruker, *SMART, SAINT and SADABS*, Bruker AXS Inc., Madison, Wisconsin, USA, 1998; (b) G. M. Sheldrick, *SHELXS-97, Program for X-ray Crystal Structure Determination*, University of Gottingen, Germany, 1997.
- 24 X. L. Zhao, X. Y. Wang, S. N. Wang, J. M. Dou, P. P. Cui, Z. Chen, D. Sun, X. P. Wang and D. F. Sun, *Cryst. Growth Des.*, 2012, **12**, 2736.
- 25 X. Feng, Y. F. Wang, Z. Q. Shi, J. J. Shang and L. Y. Wang, *Inorg. Chem. Commun.*, 2012, **22**, 131.
- 26 (a) T. P. Hu, W. H. Bi, X. Q. Hu, X. L. Zhao and D. F. Sun, *Cryst. Growth Des.*, 2010, **10**, 3324; (b) Y. Han, J.-R. Li, Y. B. Xie and G. S. Guo, *Chem. Soc. Rev.*, 2014, **43**, 5952; (c) K. C. Wang, D. W. Feng, T.-F. Liu, J. Su, S. Yuan, Y.-P. Chen, M. Bosch, X. D. Zou and H.-C. Zhou, *J. Am. Chem. Soc.*, 2014, **136**, 13983; (d) H. Reinsch, M. A. v. d. Veen, B. Gil, B. Marszalek, T. Verbiest, D. d. Vos and N. Stock, *Chem. Mater.*, 2013, **25**, 17.
- 27 (a) S. L. Li, Y. Q. Lan, J. F. Ma, Y. M. Fu, J. Yang, G. J. Ping, J. Liu and Z. M. Su, *Cryst. Growth Des.*, 2008, **8**, 1610; (b) J. Zhang, Z. J. Li, Y. Kang, J. K. Cheng and Y. G. Yao, *Inorg. Chem.*, 2004, **43**, 8085; (c) S. L. Li, Y. Q. Lan, J. F. Ma, J. Yang, G. H. Wei, L. P. Zhang and Z. M. Su, *Cryst. Growth Des.*, 2008, **8**, 675.
- 28 D. Sun, Z. H. Yan, Y. K. Deng, S. Yuan, L. Wang and D. F. Sun, *CrystEngComm.*, 2012, **14**, 7856.
- 29 (a) P. Cui, Z. Chen, D. L. Gao, B. Zhao, W. Shi and P. Cheng, *Cryst. Growth Des.*, 2010, **10**, 4370–4378; (b) X. Shi, G. S. Zhu, Q. R. Fang, G. Wu, G. Tian, R. W. Wang, D. L. Zhang, M. Xue and S. L. Qiu, *Eur. J. Inorg. Chem.*, 2004, 185; (c) L. Cui, X. J. Luan, C. P. Zhang, Y. F. Kang, W. T. Zhang, Y. Y. Wang and Q. Z. Shi, *Dalton Trans.*, 2013, **42**, 1637; (d) S. M. Fang, Q. Zhang, M. Hu, X. G. Yang, L. M. Zhou, M. Du and C. S. Liu, *Cryst. Growth Des.*, 2010, **10**, 4773; (e) Y. N. Zhang, P. Liu, Y. Y. Wang, L. Y. Wu, L. Y. Pang and Q. Z. Shi, *Cryst. Growth Des.*, 2011, **11**, 1531.
- 30 G. Blasse and B. C. Grabmaier, *Luminescent Materials*, Springer Verlag, Berlin, 1994.